Application of Parameter Estimation to Control of Reconfigurable Space Structure

Keita Sawayama, Kazuo Machida
The University of Tokyo

Takashi Matsuzawa, Toshiaki Iwata
National Institute of Advanced Industrial Science and Technology (AIST)

Yohsuke Tsutsumi
Shinwa Controls Co. Ltd.

ABSTRACT

We propose a reconfigurable space structure for the construction of such large space structures as solar power satellites. In this paper, we consider a control method for the reconfigurable space structure. We present control architecture and an application of parameter estimation. In addition, we provide an overview of a ground experimental model and some results of experiments.

再構成型宇宙構造物の制御へのパラメータ推定の適用

摘要

筆者らは，太陽発電衛星などの大型宇宙構造物の構築に再構成型宇宙構造物を利用することを提案してきた．本稿では，再構成型宇宙構造物の制御手法について考察し，再構成型宇宙構造物の制御に適したアーキテクチャの提案，パラメータ推定の手法の適用について述べる．また，地上実験装置の概要といくつかの実験結果を紹介する．

1. Introduction

Large space structures show promise for use as solar power satellites (SPSs) or space stations in the future. Many methods for the construction of large space structures have been considered, including usage of autonomous robots [1-7], space tags [8], or inflatable structures [4,9]. The usage of autonomous robots requires advanced control technology and high development cost. Moreover, the robots are not robust to failure. In the same way, the usage of space tags is difficult. On the other hand, inflatable structures are difficult to repair when hit by space debris.

To solve these problems, we propose a reconfigurable space structure [10]. The structure utilizes small satellite units and a large deployment structure. Autonomous construction is realized by autonomous docking of the satellites and the structure can be reconstructed by replacing the failed satellite unit in the case of failure. Construction utilizing autonomous docking is achieved with cooperative satellite units. At the same time, actuators (thrusters, reaction wheels) and sensors (gyros, vision sensors, etc.) on the satellite units are used not only to control themselves during the construction process but also to control the overall structure after the construction. Therefore, it is necessary that the satellite units act cooperatively. In addition, on-orbit changes of reconfigurable space structures should be considered. When the structure configuration changes, appropriate operation of the actuators also changes. Moreover, fuel consumption causes mass property change. Thus, the control architecture should be flexible to the changes and real-time estimation of the changing

mass property should be realized. Our objective is to study a cooperative and flexible control architecture that is suitable for the reconfigurable space structure. In this study, we performed simulation experiments and ground experiments using an air bearing. We introduce herein the experimental models and the results of experiments.

Section 2 gives an overview of the control architecture. In Section 3, we present an application of parameter estimation together with the results of simulation experiments. In Section 4, we present an introduction of the experimental model and the results of ground experiments. We conclude this paper in Section 5.

2. Overview of Control Architecture

The control architecture of the reconfigurable space structure should take into account cooperativity of the satellite units and flexibility to on-orbit changes. There are three approaches to realizing cooperative control: (1) centralized, (2) distributed, and (3) hybrid of (1) and (2) [11]. In the centralized approach, a central controller unit, one of the satellite units, receives sensor output from all the satellite units composing the structure. The central controller unit decides the input for all the actuators. The centralized approach achieves cooperativity but not flexibility. At the same time, the problem of computational cost will emerge when the number of satellite units increases. In the distributed approach, each satellite unit decides the control input for its own actuators based on the output from its own sensors. The distributed approach has acceptable flexibility. However, cooperativity is difficult to achieve and inconsistent action is possible, which may lead to fatal failure of the space structure. In contrast to these two approaches, the hybrid approach can satisfy both requirements of cooperativity and flexibility. The central controller unit indicates the desired motion of the overall structure to the other satellite units according to the sensor output from all the satellite units. Each satellite unit decides the input for its actuators based on the indication from the central controller unit and its own sensor output. We utilize the hybrid architecture to control the reconfigurable space structure. An overview of the architecture is shown in Fig. 1. The architecture is similar to coordination architecture for formation flight control [12]. We developed the architecture so that it would be suitable for the reconfigurable space structure in the future.

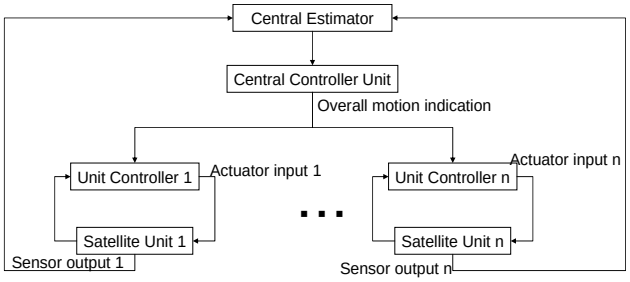

Fig. 1 Hybrid architecture for control of overall space structure

3. Application of Parameter Estimation

Mass property, center of mass position, and inertial property of the reconfigurable space structure change according to configuration change and fuel consumption after launch. Therefore, real-time estimation of mass property is desired. The estimation of mass property is considered to be a problem in estimating parameters of the motion equation. We utilize a joint filter to realize simultaneous estimation. Because satellite dynamics is nonlinear, we adopted an extended Kalman filter as the estimator [13].

We show the results of simulation experiments of parameter estimation. In the simulation, satellite attitude dynamics is taken into consideration and center of gravity (c.g.) position, moments of inertia, and products of inertia are estimated.

3.1 Estimation Algorithm

To represent the attitude, quaternion is used, so the state vector is $\mathbf{x} = \begin{bmatrix} q_1 & q_2 & q_3 & q_4 & \omega_x & \omega_y & \omega_z \end{bmatrix}^T$ and the parameter vector consists of c.g. position and inertia, $\mathbf{m} = \begin{bmatrix} x_{cg} & y_{cg} & z_{cg} & J_{xx} & J_{yy} & J_{zz} & J_{xy} & J_{yz} & J_{zx} \end{bmatrix}^T$.

The motion equation is as follows,

$$\begin{pmatrix} \dot{\mathbf{q}} \\ \dot{q}_4 \\ \dot{\boldsymbol{\omega}} \end{pmatrix} = \begin{pmatrix} -\frac{1}{2}\boldsymbol{\omega}\times\mathbf{q} + \frac{1}{2}q_4\boldsymbol{\omega} \\ \frac{1}{2}\mathbf{q}\cdot\boldsymbol{\omega} \\ \mathbf{J}^{-1}\left(\mathbf{N} - \mathbf{r}_{cg}\times\mathbf{T} - \boldsymbol{\omega}\times\mathbf{J}\boldsymbol{\omega}\right) \end{pmatrix} = \mathbf{f}(\mathbf{x},\mathbf{m}), \quad (1)$$

where $\mathbf{T}$ is thrust vector and $\mathbf{N}$ is torque vector around the origin of the body frame, and both are generated by satellite actuators. System noise vector $\mathbf{v}$ is added to $\mathbf{T}$ and $\mathbf{N}$ and it is a three-dimensional zero-mean Gaussian vector whose covariance is $\mathbf{P}_v = 1\times10^{-6}\mathbf{I}$, which is equivalent to 0.001 N or Nm. The satellite can observe attitude in Euler angle and angular velocity. The observation equation is as follows:

$$\mathbf{y} = \begin{bmatrix} \theta_x \\ \theta_y \\ \theta_z \\ \omega_x \\ \omega_y \\ \omega_z \end{bmatrix} = \begin{bmatrix} \tan^{-1}\left(\frac{2(q_2q_3+q_1q_4)}{q_3^2-q_1^2-q_2^2+q_4^2}\right) \\ \sin^{-1}(-2(q_1q_3-q_2q_4)) \\ \tan^{-1}\left(\frac{2(q_1q_2+q_3q_4)}{q_1^2-q_2^2-q_3^2+q_4^2}\right) \\ \omega_x \\ \omega_y \\ \omega_z \end{bmatrix} = \mathbf{h}(\mathbf{x}). \quad (2)$$

An observation noise vector $\mathbf{w}$ is added to the observation vector and $\mathbf{w}$ is zero-mean Gaussian whose covariance is $\mathbf{P}_w = 1\times10^{-4}\mathbf{I}$. The covariance is equivalent to 0.01 rad or rad/s error.

In the joint extended Kalman filter, the state vector and the parameter vector are augmented, $\mathbf{z} = \begin{bmatrix}\mathbf{x}^T & \mathbf{m}^T\end{bmatrix}^T$. An overview of the algorithm is shown below [13].

Initialize with

$$\hat{\mathbf{z}}_0 = E[\mathbf{z}_0], \quad (3)$$

$$\mathbf{P}_0 = E\left[(\mathbf{z}_0 - \hat{\mathbf{z}}_0)(\mathbf{z}_0 - \hat{\mathbf{z}}_0)^T\right] \quad (4)$$

The time update of the state vector is defined as $\mathbf{x}_k = \mathbf{F}(\mathbf{x}_{k-1}, \mathbf{m}_{k-1})$, which is calculated by numerical integration of eq. (1). Time-update equations of the Kalman filter are

$$\hat{\mathbf{z}}_k^- = \overline{\mathbf{F}}(\hat{\mathbf{z}}_{k-1}), \quad (5)$$

$$\mathbf{P}_k^- = \overline{\mathbf{A}}_{k-1}\mathbf{P}_{k-1}\overline{\mathbf{A}}_{k-1}^T + \mathbf{P}_v, \quad (6)$$

where

$$\overline{\mathbf{F}}(\mathbf{z}_{k-1}) = \begin{bmatrix} \mathbf{F}(\mathbf{x}_{k-1}, \mathbf{m}_{k-1}) \\ \mathbf{m}_{k-1} \end{bmatrix}, \quad (7)$$

$$\overline{\mathbf{A}}_{k-1} = \exp(\mathbf{A}_{k-1}T), \quad (8)$$

$$\mathbf{A}_{k-1} = \begin{bmatrix} \frac{\partial\mathbf{f}}{\partial\mathbf{x}}(\hat{\mathbf{x}}_{k-1}, \hat{\mathbf{m}}_{k-1}) & \frac{\partial\mathbf{f}}{\partial\mathbf{m}}(\hat{\mathbf{x}}_{k-1}, \hat{\mathbf{m}}_{k-1}) \\ \mathbf{0} & \mathbf{I} \end{bmatrix}, \quad (9)$$

and T is sample interval.

Measurement update equations are

$$\overline{\mathbf{K}}_k = \mathbf{P}_k^-\overline{\mathbf{C}}_k^T\left(\overline{\mathbf{C}}_k\mathbf{P}_k^-\mathbf{C}_k^T - \mathbf{P}_w\right), \quad (10)$$

$$\hat{\mathbf{z}}_k = \hat{\mathbf{z}}_k^- + \overline{\mathbf{K}}_k\left(\mathbf{y}_k - \mathbf{h}(\hat{\mathbf{x}}_k^-)\right), \quad (11)$$

$$\mathbf{P}_k = \left(\mathbf{I} - \overline{\mathbf{K}}_k\overline{\mathbf{C}}_k\right)\mathbf{P}_k^-, \quad (12)$$

where

$$\overline{\mathbf{C}}_k = \begin{bmatrix} \frac{\partial\mathbf{h}}{\partial\mathbf{x}}(\hat{\mathbf{x}}_k^-) & \mathbf{0} \end{bmatrix}. \quad (13)$$

3.2 Simulation Experiment

We conducted experiments for two cases: (1) $(x_{cg} \quad y_{cg} \quad z_{cg}) = (0.00 \quad 0.00 \quad 0.00)$ [m] and (2) $(x_{cg} \quad y_{cg} \quad z_{cg}) = (0.05 \quad 0.05 \quad 0.05)$ [m]. In each case, the satellite fired thrusters in +x, –x, +y, –y, +z and -z directions for 15 seconds each. The results of c.g. position estimation are shown in Fig. 2. The estimation accuracy of c.g. position is approximately 1 cm. The moments of inertia and the products of inertia are also adequately estimated.

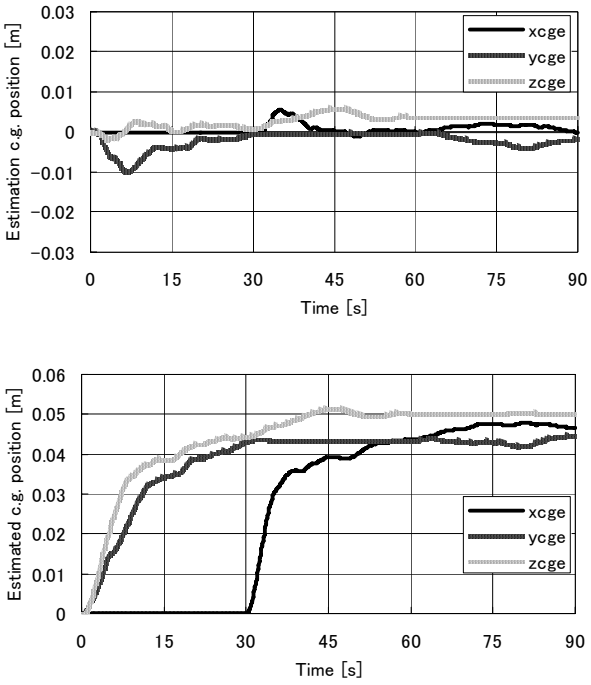

Fig. 2 Results of estimation of c.g. position. Upper: case (1) $(x_{cg} \quad y_{cg} \quad z_{cg}) = (0.00 \quad 0.00 \quad 0.00)$ [m] and lower: case (2) $(x_{cg} \quad y_{cg} \quad z_{cg}) = (0.05 \quad 0.05 \quad 0.05)$ [m].

4. Experimental Model

We show the experimental model and some results of experiments. Figure 3 shows two small satellite models. Each model measures approximately $450\,mm \times 450\,mm \times 400mm$ and weighs approximately $25\,kg$. One is a chaser satellite and the other is a target satellite. Each satellite model has an air bearing that enables it to float on the testing bench to simulate two-dimensional microgravity environment. Each satellite model has eight compressed air thrusters, one reaction wheel as actuator, and one angle, angular velocity sensor and one vision sensor (CCD camera) as sensors. The vision sensor acquires an image of the target marker on the other satellite model to detect relative position and orientation of that model. The onboard control PC is a Dell Inspiron 710m with Pentium M 735 （1.70 GHz） processor and 1 GB memory. Each satellite model has three infra-red (IR) LED markers that are observed by an overhead sensor – an IR camera positioned above the testing bench – to detect the position of the satellite on the bench. The chaser satellite model has a grapple fixture and the target satellite model has a snare-type capture mechanism as docking mechanism.

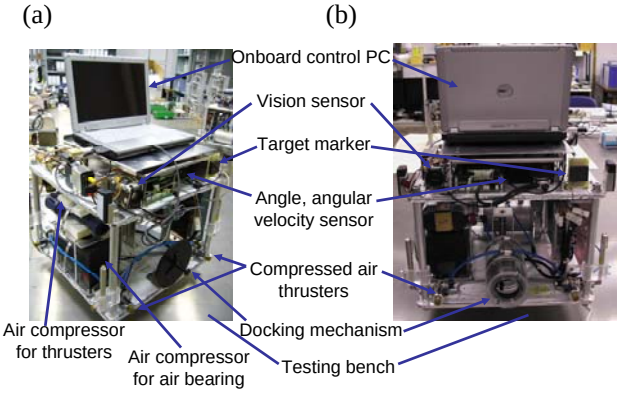

Fig. 3 Small satellite models: (a) chaser satellite and (b) target satellite

4.1 Measurement of Thruster Property

We measured a property of the compressed air thruster in relation to pulse width. Thrust of the thruster is measured with a load cell, and the results are shown in Fig. 4. Thrust derived from acceleration measurement is also shown for comparison. Both thruster properties are similar. Thrust is not proportional to pulse width and does not increase when the pulse width exceeds 50 ms. This is because pressure of the air tank drops when the pulse width becomes large.

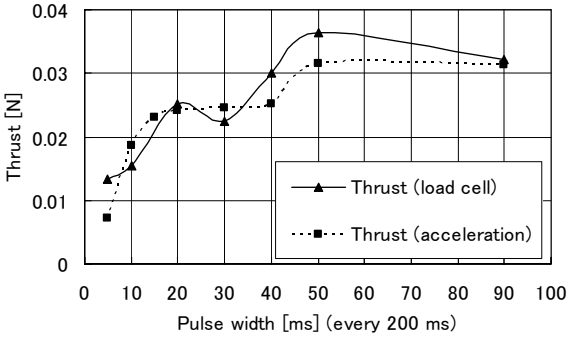

Fig. 4 Thruster property in relation to pulse width

4.2 Relative Navigation Using Vision Sensor

The vision sensor is used to obtain the relative position and attitude between satellites. Relative navigation is needed for autonomous docking during

construction and for maintaining the configuration of the overall structure.

The vision system consists of the onboard CCD camera and the target marker. The target marker is a five-point marker and is known to provide three-dimensional precise position and attitude information [14]. The outer four points are coplanar and used for position calculation. Attitude is calculated using the distance between the center of the outer four points and the prominent center point of the target marker.

The procedure to determine relative position using image processing is as follows [15]. The following explanation is about derivation of relative position in two-dimensional space.

(1) Image processing detects marker points' position in a frame coordinate, which is a two-dimensional coordinate fixed on the observed image and whose origin is the center of the image (Fig. 5).

(2) Geometrical calculation computes marker points' position in a camera frame coordinate, which is a three-dimensional coordinate whose origin is the center of the camera lens.

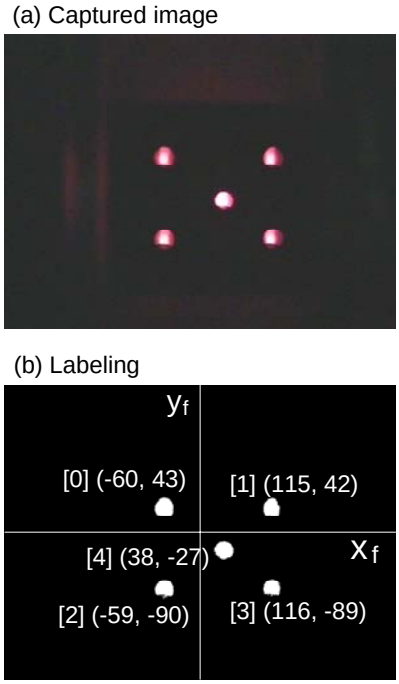

Fig. 5 Results of image processing

(3) The position and attitude of the target marker relative to the camera are calculated.

(4) Relative position of the target marker is transformed into relative position and attitude between the satellites according to the locations of the camera and the target marker on the satellites.

4.3 Autonomous Docking Mechanism Actuation

We introduce here the details of the docking mechanism and its autonomous actuation. The docking mechanism is basically the same as that used in the shuttle remote manipulator system (SRMS) or the space station remote manipulator system (SSRMS) [8, 16], and does not require precise alignment to enable connection.

Autonomous actuation of the docking mechanism with the vision system is examined experimentally. The relative position of the chaser satellite model that has a grapple fixture with respect to the target satellite model that has a capture mechanism is observed by the vision system, as described in Section 4.2. The position of the grapple fixture tip with respect to the snare-type capture mechanism is geometrically calculated from relative position and orientation observations. Once the grapple fixture tip is inserted into the snare-type capture mechanism, the onboard computer of the target satellite model immobilizes and pulls in the grapple fixture using the snare-type capture mechanism. Figure 6 shows an image of docking mechanism actuation.

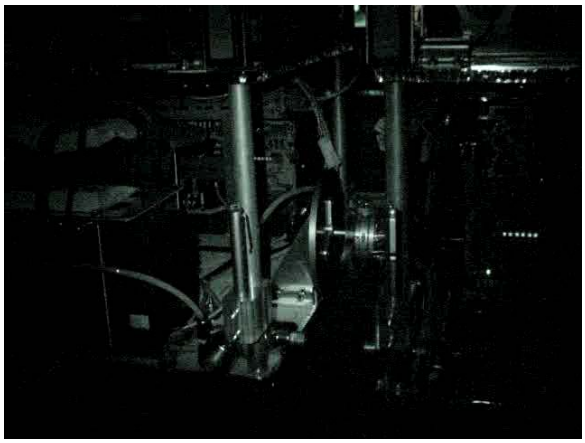

Fig. 6 Docking mechanism actuation

5. Conclusion

Our study is summarized as follows.

(1) A reconfigurable space structure for the construction of a large space structure with autonomous docking of small satellite units was introduced.

(2) Control architecture for the reconfigurable space structure is introduced. The architecture takes into account cooperativity and flexibility.

(3) An application of parameter estimation to the control of the reconfigurable space structure is considered. The results of simulation experiments are shown.

(4) A ground experimental model is introduced and the results of experiments are shown.

References

[1] M. Mori, T. Fujita, Y. Saito: "Summary of Studies on Space Solar Power Systems of Japan Aerospace Exploration Agency (JAXA)," ISTS 2006-r-1-03, 2006.

[2] H. Ueno, V. Mangalgiri, S. Dubowsky, T. Sekiguchi, M. Oda, Y. Ohkami: "Simulation, Analysis and Experiments of On-orbit Assembly Behavior on Flexible Structure by Cooperative Robots," ISTS 2004-o-2-05v, 2004.

[3] H. Ueno, M. Oda, K. Inaba: "Robotics Experimental Study for SSPS Walking and Assembly Technology," Proc. of the 8th i-SAIRAS, Munich, Germany, 2005.

[4] S. Murata, D. Jodoi, H. Furuya, Y. Terada, K. Takadama: "Conceptual Study on Inflatable Tensegrity Module for Large Scale Space Structures and Its Robotic Assembly," IAC-05-D1.1.01, 2005.

[5] V. M. Melnicov, K. M. Pichkhadze: "Design of Frameless SA Deployed by Centrifugal Forces and Its Deployment Mechanism As A Basis of New Technology of In-orbit Power Plant Assembling," IAC-05-C2.P.01, 2005.

[6] Y. Ishijima, D. Tzeranis, S. Dobowsky: "On-Orbit Maneuvering of Large Space Flexible Structures by Free-Flying Robots," Proc. of the 8th i-SAIRAS, Munich, Germany, 2005.

[7] D. Tzeranis, Y. Ishijima, S. Dobowsky: "On the Manipulation of Large Flexible Structural Modules by Robots Mounted on Large Flexible Structures," Proc. of the 8th i-SAIRAS, Munich, Germany, 2005.

[8] P. K. Ngyyen and P. C. Hughes: "Teleoperation: From the Space Shuttle to the Space Station," Teleoperation and Robotics in Space, Progress in Astronautics and Aeronautics, Vol. 161, pp. 353-410, AIAA, 1994.

[9] K. Anma, T. Kozasa, A. Tukahara, F. Takeda, T. Mori: "Development of Inflatable Truss Structure for Space Solar Power System," ISTS 2006-c-12, 2006.

[10] T. Iwata and H. Murakami: "Construction of Solar Power Satellites Using Small Satellites and Large-scale Deployable Structures," ISTS 2006-c-10, 2006.

[11] G. A. Bekey: "Autonomous Robots: From Biological Inspiration to Implementation and Control," MIT Press, 2005.

[12] R. W. Beard, J. L. Lawton, F. Y. Hadaegh: "A Coordination Architecture for Spacecraft Formation Control," IEEE Transactions on Control Systems Technology, Vol. 9, No. 6, pp. 777-790, 2001.

[13] E. A. Wan and A. T. Nelson: "Kalman Filtering and Neural Networks, ch. 5, Dual Extended Kalman Filter Methods," Wiley, 2001.

[14] W. Fehse: "Autonomous Rendezvous and Docking of Spacecraft," Cambridge University Press, 2003.

[15] K. Sawayama, et al.: "Autonomous Docking of Small Satellites in Large Space Structure", IAC-07-C1-I-09, 2007.

[16] B. Walker and R. Vandersluis: "Design, Testing and Evaluation of Latching End Effector," Proceedings of the 29th Aerospace Mechanism Symposium, pp. 1-16, NASA Conference Publication 3293, 1995.